Organic & Biomolecular Chemistry

This article is part of the

OBC 10th anniversary

themed issue

All articles in this issue will be gathered together online at

www.rsc.org/OBC10

Organic & Biomolecular Chemistry

Cite this: *Org. Biomol. Chem.*, 2012, **10**, 5787

www.rsc.org/obc

COMMUNICATION

Short polyglutamine peptide forms a high-affinity binding site for thioflavin-T at the N-terminus†‡

Shigeru Matsuoka,*[a,b] Motoki Murai,[a] Toshio Yamazaki[c] and Masayuki Inoue*[a]

Received 22nd December 2011, Accepted 23rd February 2012
DOI: 10.1039/c2ob07157f

Thioflavin-T is one of the most important amyloid specific dyes and has been used for more than 50 years; however, the molecular mechanism of staining is still not understood. Chemically synthesized short polyglutamine peptides (Q_n, n = 5–10) were subjected to the thioflavin-T (ThT) staining assay. It was found that the minimum Q_n peptide that stained positive to ThT was Q_6. Two types of ThT-binding sites, a high-affinity site (k_{d1} = 0.1–0.17 μM) and a low-affinity site (k_{d2} = 5.7–7.4 μM), were observed in short polyQs (n = 6–9). $^{13}C\{^2H\}$REDOR NMR experiments were carried out to extract the local structure of ThT binding sites in Q_8 peptide aggregates by observing the intermolecular dipolar coupling between [3-Me-d_3]ThT and natural abundance Q_8 or residue-specific [1,2-$^{13}C_2$] labeled Q_8s. $^{13}C\{^2H\}$ REDOR difference spectra of the [3-Me-d_3]ThT/natural abundance Q_8 (1/9) complex indicated that all of the five carbons of the glutamine residue participated in the formation of ThT-binding sites. $^{13}C\{^2H\}$DQF–REDOR experiments of [3-Me-d_3]ThT/residue-specific [1,2-$^{13}C_2$] labeled Q_8 (1/50) complexes demonstrated that the N-terminal glutamine residue had direct contact with the ThT molecule at the high-affinity ThT-binding sites.

Thioflavin-T (ThT, **1**, Fig. 1), a cationic derivative of benzothiazole aniline, was reported to be a fluorescent stain for amyloid in 1959.[1] This compound has been widely used in basic research and diagnosis of amyloid as one of the gold-standard dyes for amyloid staining for more than 50 years.[2,3] However, in spite of its extensive application, the precise molecular mechanism of the staining remains unclear. Insoluble amyloid, a fibrous β-sheet rich aggregate, is formed by various types of proteins. For instance, more than forty human proteins are known to form amyloid-like fibrils, and cause conformational diseases such as Alzheimer's, Parkinson's, Huntington's and prion diseases.[4] Interestingly, all of these protein aggregates, which possess distinct amino acid sequences, are similarly stained by the common amyloid-specific dyes, ThT and Congo-red.[5] Therefore, the molecular recognition between these dyes and the peptides exhibits both selectivity for aggregates and tolerance to different amino acid sequences. To understand these peculiar binding characteristics, it is necessary to elucidate the dye–amyloid complex structure at atomic resolution.[6]

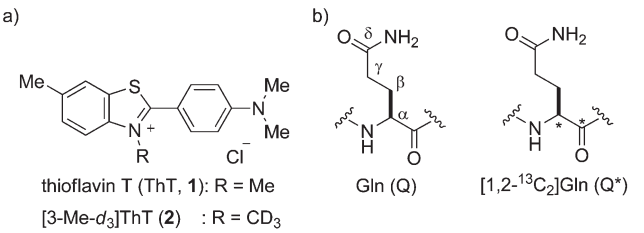

Fig. 1 (a) Chemical structures of thioflavin T (**1**) and [3-Me-d_3]ThT (**2**). (b) Structure of glutamine (Q) residue. The labeled positions of [1,2-$^{13}C_2$]glutamine (Q*) are indicated by asterisks.

It has been a significant challenge to study the dye–peptide complex structure due to insolubility and heterogeneity of the peptide aggregates. Furthermore, potential multiplicity of the binding modes and low concentration of the binding sites in fibrils make the situation even more problematic.[7] Because of these issues, only computational simulations of the dye–peptide complex molecular structure have been reported,[8] and partial structural insight of the complex has been disclosed by several X-ray diffraction studies of the dye–non-fibrillar protein cocrystals.[9]

In this communication, we report the first observation of direct molecular contacts between ThT and model peptide aggregates by applying solid-state NMR spectroscopy. As a model for ThT-stainable peptide aggregates, polyglutamine (polyQ) peptides were employed, because the polyQ motif has an intrinsic tendency toward aggregation and a correlation with polyglutamine diseases.[10]

Although a number of polyQ model peptides were reported to form amyloid-like fibrils,[11] the threshold number of the

[a]*Graduate School of Pharmaceutical Sciences, The University of Tokyo, 7-3-1 Hongo, Bunkyo-ku, Tokyo 113-0033, Japan. E-mail: inoue@mol.f.u-tokyo.ac.jp; Fax: +81-35841-0568; Tel: +81-35841-1354*
[b]*JST, ERATO, Lipid Active Structure Project, Toyonaka, Osaka 560-0043, Japan. E-mail: matsuokas11@chem.sci.osaka-u.ac.jp; Fax: +81-66850-6607; Tel: +81-66850-6605*
[c]*RIKEN System and Structural Biology Center, 1-7-22 Suehiro-cho, Tsurumi-ku, Yokohama 230-0045, Japan*

†This article is part of the *Organic & Biomolecular Chemistry* 10th Anniversary issue.

‡Electronic supplementary information (ESI) available. See DOI: 10.1039/c2ob07157f

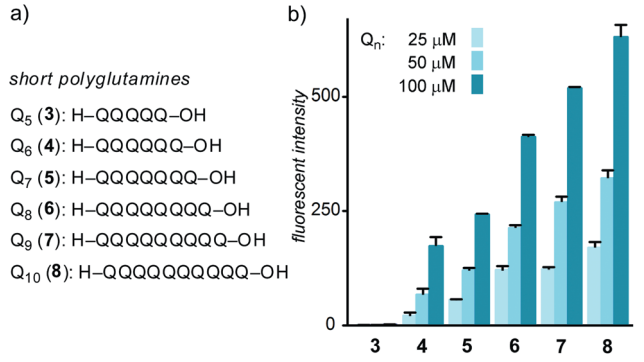

Fig. 2 (a) Six short polyglutamines were synthesized as C- and N-terminal free peptides. (b) Et_2O precipitates of short polyglutamines (**3**–**8**) were subjected to ThT-staining. The threshold residue number for Q_n to form ThT stainable aggregates was $n = 6$; above that, characteristic fluorescent emission from bound-ThT was observed were performed with 5 μM of ThT at three different concentrations of Q_n (25, 50 and 100 μM) in glycine buffer solution pH 8.7 at 27 °C. Fluorescence from bound-ThT was measured at ex440 nm and em470 nm.[3]

Table 1 Dissociation constants and number of ThT-binding sites of Q_n peptides[a]

Peptide	k_{d1}/μM	$N_1/10^{-3}$	k_{d2}/μM	$N_2/10^{-3}$
4	0.17	20.1	6.45	77.7
5	0.11	19.4	5.72	65.0
6	0.10	21.7	6.76	86.3
7	0.15	25.1	7.42	82.4

[a] Two distinct binding sites were observed with higher affinity (K_{d1}, N_1) and lower affinity (K_{d2}, N_2). N is the number of binding sites for one Q_n molecule.

glutamine residues required for formation of aggregates was not determined. To simplify the structural analysis of the complex, we decided to first elucidate the minimum ThT-stainable polyQ lengths. Accordingly, a series of short polyQs, **3**–**8** (Fig. 2a), were synthesized by Fmoc solid phase peptide synthesis, and the products were treated with diethylether to precipitate the corresponding aggregates. The aggregates were insoluble in both water and various organic solvents, except for Q_5 (**3**), which was water soluble. X-ray diffraction studies of the aggregates clearly indicated that Q_6–Q_{10} (**4**–**8**) mainly contained β-sheets, the typical secondary structure of amyloid fibrils.[12]

The formation of ThT-binding sites in Q_5–Q_{10} (**3**–**8**) was evaluated by the ThT fluorescent staining assay (Fig. 2b).[3] Synthetic polyQs longer than six residues (**4**–**8**) possessed considerably enhanced ThT fluorescence with excitation and emission maxima at 440 nm and 470 nm respectively, at the three different concentrations studied. The results indicated formation of ThT-binding sites in the insoluble aggregates of **4**–**8**. According to Scatcherd analysis of **4**–**7**,[13] similar high- and low-affinity ThT binding sites were found in all the aggregates (Table 1). Numbers and the affinities of the two binding sites were inconsequential to the length of the peptides. The high-affinity sites (k_{d1} = 0.1–0.17 μM) were composed of approximately 50 peptides, while *ca.* 12 peptides were necessary for the formation of the low-affinity sites (k_{d2} = 5.7–7.4 μM). Most importantly, the dissociation constants of these binding sites were in the same order of magnitude as those found in biological amyloids, suggesting that the aggregates **4**–**7** functioned as model systems for the structural analyses of the ThT-stained polyQ amyloids.[14]

Next, we turned our attention to the direct structural analysis of the molecular contacts between ThT and Q_8 (**6**) by applying rotational-echo double-resonance (REDOR) NMR spectroscopy.[15] To do so, deuterated ThT ([3-Me-d_3]ThT (**2**)) was designed and synthesized as a suitable probe for extraction of the local structure in the sample. Indeed ^{2}H has the lowest natural abundance among NMR-active isotopes of the six most common elements (CHONPS) in biological systems. ^{13}C-observed ^{2}H-dephased REDOR (^{13}C{^{2}H}REDOR) experiments were utilized to detect the proximity between ^{13}C nuclei of **6** to the Me-d_3 group of **2** by observing intermolecular ^{13}C–^{2}H dipolar coupling (Fig. 3).[16] ^{13}C{^{2}H}REDOR experiments were carried out as a pair of ^{13}C NMR spectra with ^{2}H irradiation (REDOR: S) and without ^{2}H irradiation (full-echo: S_0). The spatial approximation between ^{13}C and ^{2}H was detected as the decay of the ^{13}C signal in the S spectrum according to the size of the restored ^{13}C–^{2}H dipolar coupling, which is inversely proportional to the cube of the interatomic distance between ^{13}C and ^{2}H. Therefore, NMR signals of ^{13}Cs in close proximity from ^{2}H dephaser can be extracted by taking the difference spectrum $S_0 - S$ (REDOR difference, ΔS).

First, 50 μM of **2** was mixed with 100 μM of Q_8 (**6**) in a ratio of 1/9 mol/mol (ThT/peptide) in aqueous buffer, and then the solution was lyophilized. Under these conditions, both high-affinity and low-affinity sites were occupied. The resulting powder sample was used in the solid state NMR measurement. The ^{13}C NMR spectrum of the **2/6** complex was measured as a full echo S_0 spectrum shown in Fig. 3, bottom. Resonances arising from natural abundance ^{13}C gave five resolved peaks of the glutamine unit (C^α, C^β, C^δ, C^γ, and C=O); however, all eight residues were overlapped. ^{13}C chemical shifts of C=O and C^α corresponded to those in a β-sheet structure.[17]

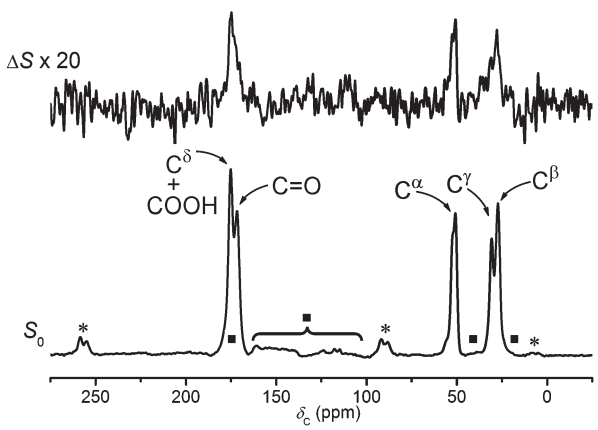

Fig. 3 ^{13}C{^{2}H}REDOR spectra of [3-Me-d_3]ThT (**2**)/Q_8 (**6**) (1/9 mol/mol) complex. Full-echo ^{13}C NMR spectrum (S_0) is shown at the bottom and REDOR difference (ΔS) is shown on the top with 20× magnification. Spectra were recorded with a dephasing time of 9.6 ms (80 rotor cycles) at a MAS speed of 8333 Hz. The number of scans was175 000. Signals arisen from ThT are marked by filled squares. The spinning side bands are marked with an asterisk.

The $^{13}C\{^{2}H\}$REDOR difference spectrum ΔS of **2/6** complex is shown in Fig. 3, top. For efficient selective observation of ^{13}C nuclei adjacent to the CD_3 group, 9.6 ms of dephasing time was applied to obtain the maximum REDOR dephasing for ^{13}C nuclei within 3.1 Å from the center of three deuterons.[18] All five ^{13}Cs gave ΔS signals in the difference spectrum with intensities over 2% of S_0, which indicated that the five carbon atoms of the glutamine unit were in proximity to **2** through participation in the high- and/or low-affinity binding sites. However, determination of the specific residue that neighbored **2** was not possible due to the signal overlap among the eight glutamine residues of **6**.

To assign the ThT-contacting residue, a series of eight residue-specific $^{13}C_2$-labeled Q_8s **9–16** were prepared by incorporating the asymmetrically synthesized [1,2-$^{13}C_2$]Gln (Fig. 1b and 4), and subjected to the solid-state NMR study. The extraction of ^{13}C NMR signals from a particular residue was achieved by combination of residue-specific labeling by [1,2-$^{13}C_2$]Gln and ^{13}C–^{13}C pair selection by double-quantum filtering (DQF) to suppress the large background signals arising from natural abundance ^{13}Cs of the other seven Gln residues.[19] For specific analysis of the local structure of the high-affinity sites, the concentration of **2** was lowered in these experiments. Namely, residue specific labeled Q_8 peptides **9–16** were incubated with **2** at a ratio of 1/50 mol/mol (ThT/peptide), where ThT molecules and the number of high-affinity binding sites were equivalent, and then frozen with liquid nitrogen to be lyophilized.

The in-phase DQF spectra were measured for each of **9–16**. Naturally abundant ^{13}C signals from the side chain C^{β}, C^{γ}, and C^{δ} were sufficiently suppressed in the DQF spectra; consequently, only the signals from the main chain $^{13}C^{\alpha}$ and $^{13}C{=}O$ of [1,2-$^{13}C_2$]Gln were selectively observed (Fig. 4 and 5).[20]

With the residue-selected DQF spectra of **9–16** in hand, we undertook assignment of the glutamine residue contacting the ^{2}H by $^{13}C\{^{2}H\}$DQF–REDOR experiments (Fig. 5b).[21] Intriguingly, only ^{13}C DQF signals of **2/9**, which has the $^{13}C^{\alpha}$–$^{13}C{=}O$ unit at the first residue from the N-terminus, exhibited a detectable REDOR difference in ΔS when dephased by the 3-CD_3 group of **2**. Thus, in terms of proximity to the CD_3 group of ThT, the N-terminal glutamine residue contacts **2**. Since the chemical shifts

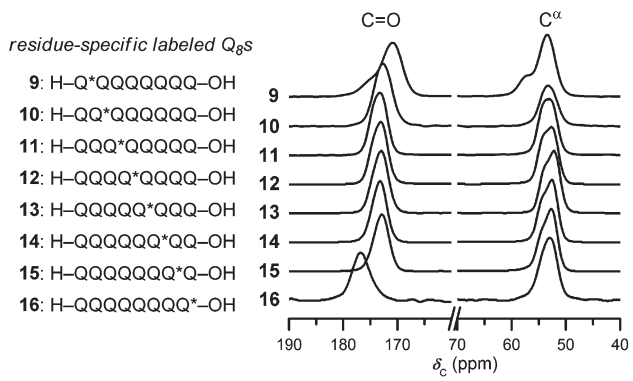

Fig. 4 ^{13}C DQF spectra of residue-specific [1,2-$^{13}C_2$] labeled Q_8s. The labeled positions are shown on the left and the DQF spectra are shown on the right. The ^{13}C–^{13}C bilinear term was evolved and refocused for 9.6 ms (80 T_r).

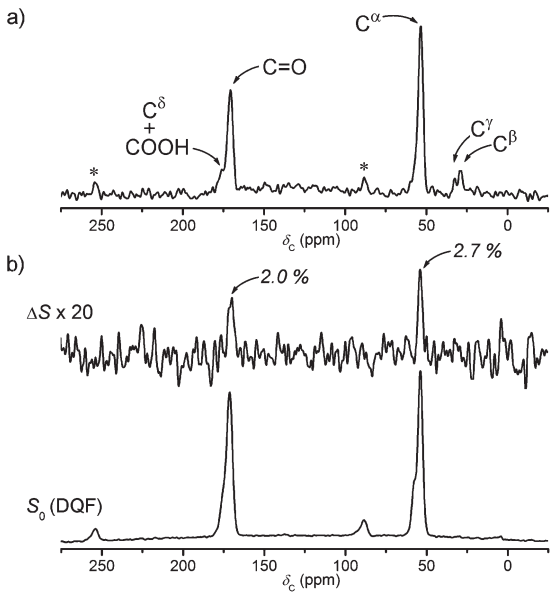

Fig. 5 (a) ^{13}C CP-MAS spectrum of [3-Me-d_3]ThT (**2**)/Q*Q_7 (**9**) (1/50 mol/mol). (b) $^{13}C\{^{2}H\}$DQF–REDOR spectra of the **2/9** (1/50 mol/mol) complex. DQF full-echo ^{13}C NMR spectrum (S_0) is shown at the bottom and REDOR difference (ΔS) is shown on the top with 20× magnification. Spectra were recorded with a dephasing time of 9.6 ms (80 rotor cycles) at a MAS speed of 8333 Hz. The number of scans was 100 000. The spinning side bands are marked with an asterisk.

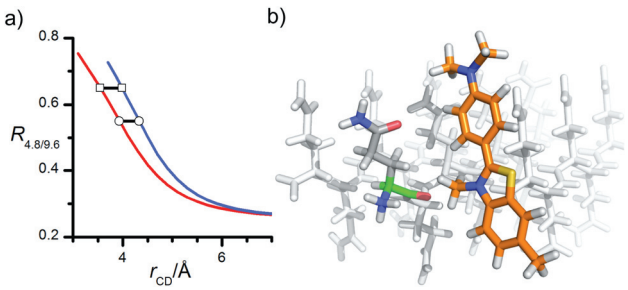

Fig. 6 (a) Ratio of $\Delta S/S_0$ between two dephasing times, 4.8 ms and 9.6 ms, plotted against the C–CD_3 interatomic distance (r_{CD}). The solid lines show the simulated values for the shortest (red) and the longest (blue) case.[22] The open square and open circle show the experimental results of **2/9** (1/9 mol/mol) complex obtained for C=O (0.65) and C^{α} (0.55) respectively. (b) Schematic diagram of ThT–Q_8 aggregate complex structure. The Q_8 aggregate is shown as an antiparallel β-sheet (white). The N-terminal Q residue is presented in atom-coded colors (C: grey, H: white, O: red, N: blue, ^{13}C: green). According to REDOR distance constraints,[22] ThT (orange) was placed to avoid steric repulsions with the Q_8 aggregate.

of $^{13}C^{\alpha}$–$^{13}C{=}O$ in the ΔS spectrum corresponded to a β-sheet structure, the first glutamine residue of Q_8 forming the ThT-binding sites also participated in the β-sheet structure.

To gain a quantitative understanding of interatomic distances between the CD_3 group of **2** and the $^{13}C^{\alpha}$–$^{13}C{=}O$ unit of **9**, REDOR difference spectra were measured at two different dephasing times, 4.8 ms and 9.6 ms, for the **2/9** complex. Fig. 6a shows a plot of $R_{4.8/9.6}$, the ratio of $\Delta S/S_0$ between the two dephasing times, against the C–CD_3 distance. When the

C–CD_3 distance (r_{CD}) is longer than the van der Waals contact range (>3.12 Å) and $R_{4.8/9.6}$ is less than 1, the value of $R_{4.8/9.6}$ has a one-to-one correspondence with the C–CD_3 distance and thus can be used for distance estimation. Assuming a single distance component, the C–CD_3 distances were deduced to be 3.6–4.0 Å and 3.9–4.3 Å for C═O ($R_{4.8/9.6}$ = 0.65) and C^{α} ($R_{4.8/9.6}$ = 0.55), respectively. Using the distance constraints from the second residue (no detectable REDOR dephasing for **2**/**10**) as well as avoiding contact within the van der Waals surfaces of **2** and Q_8, the possible geometry of CD_3 in relation to the polyglutamine residue was estimated as shown in Fig. 6b.[22] This model indicated that the high-affinity ThT-binding site in the Q_8 aggregate was located at the gap in the β-sheet structure where the N-terminal Q residue has a hydrogen bonding partner only on one face. The geometry of the CD_3 group implied the presence of a CH_3···O═C interaction between the 3-methyl group of ThT and the main chain carbonyl group of the N-terminal Q residue, which may be one of the possible interactions stabilizing the ThT–Q_8 complex at the high-affinity binding site.[23]

In conclusion, we synthesized various short polyQs (Q_6–Q_{10}), determined the minimum peptide stained by the amyloid specific dye ThT to be Q_6, and observed the intermolecular contacts between ThT and Q_8 by REDOR NMR spectroscopy. The short polyglutamine aggregates possessed β-sheet rich structures, and their high- and low-affinity binding sites corresponded to the same order of binding affinity as those formed in natural amyloids. Eight residue-specific labeled Q_8(*n*-[1,2-$^{13}C_2$]Gln) peptides were synthesized and mixed with [3-Me-d_3]ThT for the solid-state NMR measurements. $^{13}C\{^2H\}$DQF–REDOR experiments of these residue specific labeled samples successfully resulted in the assignment of the N-terminal residue that was in direct contact with ThT at the high-affinity binding site. Although the peptides used in this study were a simplified model, the strategy employed here to obtain precise local structural information should be generally applicable to binding sites in other amyloids, and studies along this line are currently ongoing.

This research was financially supported by the Funding Program for Next Generation World-Leading Researchers (M.I.) and Grant-in-Aids for Young Scientists (start up) (S.M.).

Notes and references

1 P. S. Vassar and C. F. A. Culling, *Arch. Path.*, 1959, **68**, 487–498.
2 (*a*) A. J. Howie and D. B. Brewer, *Micron*, 2009, **40**, 285–301; (*b*) C. A. Mathis, Y. Wang and W. E. Klunk, *Curr. Pharm. Des.*, 2004, **10**, 1469–1492.
3 H. LeVine III, *Methods Enzymol.*, 1999, **309**, 274–284.
4 (*a*) R. W. Carrell and D. A. Lomas, *Lancet*, 1997, **350**, 134–138; (*b*) T. Scheibel and J. Buchner, *Handb. Exp. Pharmacol.*, 2006, **172**, 199–219.
5 (*a*) P. Westermark, M. D. Benson, J. N. Buxbaum, A. S. Cohen, B. Frangione, S. Ikeda, C. L. Masters, G. Merlini, M. J. Saraiva and J. D. Sipe, *Amyloid*, 2005, **12**, 1–4; (*b*) M. Fändrich, *Cell. Mol. Life Sci.*, 2007, **64**, 2066–2078.
6 For review, see: (*a*) A. A. Reinke and J. E. Gestwicki, *Chem. Biol. Drug Des.*, 2011, **77**, 399–411; (*b*) M. Biancalana and S. Koide, *Biochim. Biophys. Acta*, 2010, **1804**, 1405–1412; (*c*) M. Groenning, *J. Chem. Biol.*, 2010, **3**, 1–18.
7 H. Levine III, *Amyloid*, 2005, **12**, 5–14.
8 (*a*) C. Wu, Z. Wang, H. Lei, Y. Duan, M. T. Bowers and J. E. Shea, *J. Mol. Biol.*, 2008, **384**, 718–729; (*b*) C. Wu, M. T. Bowers and J. E. Shea, *Biophys. J.*, 2011, **100**, 1316–1324.
9 (*a*) M. Harel, B. Cusack, J. L. Johnson, I. Silman, J. L. Sussman and T. L. Rosenberry, *J. Am. Chem. Soc.*, 2008, **130**, 7856–7861; (*b*) M. Biancalana, K. Makabe, A. Koide and S. Koide, *J. Mol. Biol.*, 2009, **385**, 1052–1063; (*c*) L. S. Wolfe, M. F. Calabrese, A. Nath, D. V. Blaho, A. D. Miranker and Y. Xiong, *Proc. Natl. Acad. Sci. U. S. A.*, 2010, **107**, 16863–16868.
10 (*a*) M. Viau, M. Létourneau, A. Sirois-Deslongchamps, Y. Boulanger and A. Fournier, *Biopolymers*, 2007, **88**, 754–763; (*b*) H. T. Orr and H. Y. Zoghbi, *Annu. Rev. Neurosci.*, 2007, **30**, 575–621.
11 (*a*) R. H. Walters and R. M. Murphy, *J. Mol. Biol.*, 2009, **393**, 978–92; Intensive study on model peptide $K_2Q_nK_2$ has been performed by Wetzel *et al.*, for example: (*b*) S. Chen, V. Berthelier, J. B. Hamilton, B. O'Nuallain and R. Wetzel, *Biochemistry*, 2002, **41**, 7391–7399; (*c*) D. Sharma, L. M. Shinchuk, H. Inouye, R. Wetzel and D. A. Kirschner, *Proteins: Struct., Funct., Bioinf.*, 2005, **61**, 398–411; (*d*) K. Kar, M. Jayaraman, B. Sahoo, R. Kodali and R. Wetzel, *Nat. Struct. Mol. Biol.*, 2011, **18**, 328–36.
12 The characteristic 4.8 Å reflection, which is attributed to the strand spacing within β-sheet layers, was observed. X-ray diffraction patterns are shown in the ESI as Fig. S2.‡ We thank Dr Yuya Koike (Radioisotope Center, The University of Tokyo) for help in measurement of X-ray diffraction.
13 Experimental results were shown as a Scatcherdplot (Fig. S3) in the ESI.‡.
14 The affinity of ThT towards various types of amyloide has been reported to be 0.033 to 23 μM. For details, see ref. 6c and references therein.
15 (*a*) T. Gullion and J. Schaefer, *Adv. Magn. Reson.*, 1989, **13**, 58–83; For reviews, see (*b*) J. Schaefer, in *Recent Trends in Molecular Recognition*, ed. F. Diederich and H. Kunzer, Springer, Berlin, 1998, 26–52; (*c*) S. L. Grage and A. Watts, *Annu. Rep. NMR Spectrosc.*, 2006, **60**, 191–228; (*d*) T. Gullion, *Annu. Rep. NMR Spectrosc.*, 2009, **65**, 111–137; (*e*) S. Matsuoka and M. Inoue, *Chem. Commun.*, 2009, 5664–5675; (*f*) O. Toke and L. Cegelski, in *Solid-State NMR Studies of Biopolymers*, ed. A. E. McDermott and T. Polenova, Wiley, New York, 2010, pp. 473–490.
16 (*a*) A. Schmidt, T. Kowalewski and J. Schaefer, *Macromolecules*, 1993, **26**, 1729–1733; (*b*) P. L. Lee and J. Schaefer, *Macromolecules*, 1995, **28**, 1921–1924; (*c*) M. E. Merritt, J. M. Goetz, D. Whitney, C.-P. P. Chang, L. Heux, J. L. Halary and J. Schaefer, *Macromolecules*, 1997, **31**, 1214–1220; (*d*) T. Gullion, *J. Magn. Reson.*, 1999, **139**, 402–407; (*e*) R. D. O'Connor, J. A. Byers, W. D. Arnold, E. Oldfied, K. L. Wooley and J. Schaefer, *Macromolecules*, 2002, **35**, 2618–2623; (*f*) S. D. Cady, J. Wang, Y. Wu, W. F. Degrado and M. Hong, *J. Am. Chem. Soc.*, 2011, **133**, 4274–4284; (*g*) S. A. Luthra, M. Utz, E. M. Gorman, M. J. Pikal, E. J. Munson and J. W. Lubach, *J. Pharm. Sci.*, 2012, **101**, 283–290.
17 (*a*) D. S. Wishart and B. D. Sykes, *J. Biomol. NMR*, 1994, **4**, 171–180; (*b*) D. S. Wishart, *Prog. Nucl. Magn. Reson. Spectrosc.*, 2011, **58**, 62–87.
18 The size of REDOR dephasing ($\Delta S/S_0$) for different dephasing time is shown in the ESI as Fig. S9.‡.
19 (*a*) A. Lesage, M. Bardet and L. Emsley, *J. Am. Chem. Soc.*, 1999, **121**, 10987–10993; (*b*) R. Verel, J. D. van Beek and B. H. Meier, *J. Magn. Reson.*, 1999, **140**, 300–303; (*c*) L. J. Mueller, D. W. Elliott, G. M. Leskowitz, J. Struppe, R. A. Olsen, K.-C. Kim and C. A. Reed, *J. Magn. Reson.*, 2004, **168**, 327–335.
20 The chemical shifts of all of Cα and amide C═O of **9–16** correspond to those observed for the β-sheet structure, except for the carboxylic acid C═O of **16**.
21 S. Matsuoka and J. Schaefer, *J. Magn. Reson.*, 2006, **183**, 252–258.
22 Detailed distance restraints are shown in the ESI.‡.
23 (*a*) J. Zhang, H. Sato, H. Tsuji, I. Noda and Y. Ozaki, *Macromolecules*, 2005, **38**, 1822–1828; (*b*) J. Zhang, H. Sato, H. Tsuji, I. Noda and Y. Ozaki, *J. Mol. Struct.*, 2005, **735–736**, 249–257.

